At the Limits of Criticality-Based Quantum Metrology: Apparent Super-Heisenberg Scaling Revisited

Marek M. Rams,[1,*] Piotr Sierant,[1,†] Omyoti Dutta,[1,2] Paweł Horodecki,[3,‡] and Jakub Zakrzewski[1,4,§]

[1]*Instytut Fizyki im. Mariana Smoluchowskiego, Uniwersytet Jagielloński, Łojasiewicza 11, 30-348 Kraków, Poland*

[2]*Donostia International Physics Center DIPC, Paseo Manuel de Lardizabal 4, 20018 Donostia-San Sebastián, Spain*

[3]*Faculty of Applied Physics and Mathematics, Gdańsk University of Technology, Gabriela Narutowicza 11/12, 80-233 Gdańsk, Poland and National Quantum Information Center of Gdańsk, Władysława Andersa 27, 81-824 Sopot, Poland*

[4]*Mark Kac Complex Systems Research Center, Uniwersytet Jagielloński, Kraków 30-348, Poland*

(Received 6 May 2017; revised manuscript received 19 February 2018; published 19 April 2018)

We address the question of whether the super-Heisenberg scaling for quantum estimation is indeed realizable. We unify the results of two approaches. In the first one, the original system is compared with its copy rotated by the parameter-dependent dynamics. If the parameter is coupled to the one-body part of the Hamiltonian, the precision of its estimation is known to scale at most as N^{-1} (Heisenberg scaling) in terms of the number of elementary subsystems used N. The second approach compares the overlap between the ground states of the parameter-dependent Hamiltonian in critical systems, often leading to an apparent super-Heisenberg scaling. However, we point out that if one takes into account the scaling of time needed to perform the necessary operations, i.e., ensuring adiabaticity of the evolution, the Heisenberg limit given by the rotation scenario is recovered. We illustrate the general theory on a ferromagnetic Heisenberg spin chain example and show that it exhibits such super-Heisenberg scaling of ground-state fidelity around the critical value of the parameter (magnetic field) governing the one-body part of the Hamiltonian. Even an elementary estimator represented by a single-site magnetization already outperforms the Heisenberg behavior providing the $N^{-1.5}$ scaling. In this case, Fisher information sets the ultimate scaling as $N^{-1.75}$, which can be saturated by measuring magnetization on all sites simultaneously. We discuss universal scaling predictions of the estimation precision offered by such observables, both at zero and finite temperatures, and support them with numerical simulations in the model. We provide an experimental proposal of realization of the considered model via mapping the system to ultracold bosons in a periodically shaken optical lattice. We explicitly derive that the Heisenberg limit is recovered when the time needed for preparation of quantum states involved is taken into account.

DOI: 10.1103/PhysRevX.8.021022

Subject Areas: Quantum Physics, Quantum Information

I. INTRODUCTION

At the center of quantum metrology [1–4] lies the concept of estimation of a small external parameter with the help of a quantum procedure. The main idea is to engineer a family of quantum states depending strongly on that parameter in the sense that a small difference in the parameter value makes the states significantly different from each other. The relevant quantifier of a distance between quantum states is the quantum fidelity [5],

$$\mathcal{F}(\hat{\rho},\hat{\sigma}) = \mathrm{Tr}\left(\sqrt{\sqrt{\hat{\rho}}\hat{\sigma}\sqrt{\hat{\rho}}}\right), \tag{1}$$

where density operators $\hat{\rho}$ and $\hat{\sigma}$ describe the states being compared.

Now consider a family of quantum states $\hat{\rho}(\lambda)$ controlled by a parameter λ and let δ_λ be a small shift of the parameter that we want to estimate. An ultimate bound on the

*marek.rams@uj.edu.pl
†piotr.sierant@uj.edu.pl
‡pawel@mif.pg.gda.pl
§jakub.zakrzewski@uj.edu.pl

accuracy of any estimate one may make on the unknown δ_λ is set be the quantum Fisher information (QFI) [3,6]:

$$G(\lambda) = -4\partial^2\mathcal{F}[\hat{\rho}(\lambda), \hat{\rho}(\lambda+\delta_\lambda)]/\partial\delta_\lambda{}^2|_{\delta_\lambda=0}. \quad (2)$$

Indeed, in order to identify δ_λ one has to measure some observable $\hat{A}$, called an estimator. The precision it offers is quantified by the error propagation formula given by the inverse of signal-to-noise ratio:

$$\Delta_{\delta_\lambda}(\hat{A}, \lambda) = \frac{\sqrt{\langle \hat{A}^2\rangle_{\rho(\lambda)} - \langle \hat{A}\rangle^2_{\rho(\lambda)}}}{\left|\frac{\partial\langle\hat{A}\rangle_{\rho(\lambda+\delta_\lambda)}}{\partial\delta_\lambda}\Big|_{\delta_\lambda=0}\right|}. \quad (3)$$

The ultimate lower bound for the uncertainty of estimation of the small deviation δ_λ is set by the quantum Cramer-Rao bound [3],

$$\Delta_{\delta_\lambda}(\hat{A}, \lambda) \geq G(\lambda)^{-1/2}, \quad (4)$$

which is independent of the observable $\hat{A}$ and determined by the QFI. In principle, the above bound would be saturated by the measurement projecting on the eigenvectors of the so-called symmetric logarithmic derivative operator $\hat{\mathcal{L}}$, satisfying $2[\partial\hat{\rho}(\lambda)/\partial\lambda] = \hat{\mathcal{L}}\hat{\rho}(\lambda) + \hat{\rho}(\lambda)\hat{\mathcal{L}}$. In practice, however, an identification of an appropriate symmetric logarithmic derivative operator is a formidable task in itself. For a quite general class of systems we show that there exists the observable yielding a correct scaling with the system size in appropriate limits.

There are basically two different scenarios discussed in the literature on how to introduce the dependence of the state on the parameter δ_λ. In the first approach [7–9] the state is rotated by some Hamiltonian and then the estimator observable $\hat{A}$ is measured—providing the accuracy that is determined by the error propagation formula. Let us call it a rotation scenario.

In principle, with a many-body interacting Hamiltonian the corresponding Fisher information could have implied the error vanishing exponentially with N [10]. It has been proven, however, that when the Hamiltonian is composed only of local on-site (or one-body, see, e.g., Ref. [11]) terms $\hat{h}_n$, i.e.,

$$\hat{H} = \lambda\hat{H}_1 = \lambda\sum_{n=1}^{N}\hat{h}_n, \quad (5)$$

then at most $G^{-1/2} \sim N^{-1}$. Such a scaling is referred to as the Heisenberg limit and should be contrasted with the classical type of behavior where $G^{-1/2} \sim N^{-1/2}$, i.e., the shot-noise limit. It has been argued that adding to the above Hamiltonian other interactions—not coupled to λ—cannot improve the scaling beyond the Heisenberg limit [11–16]. Furthermore, let us mention that the final formula is quite sensitive to a local noise, and because of that, one basically always ends up with the classical scaling for large enough N [17].

More precisely, bringing the time of the evolution explicitly into the picture, for the Hamiltonian of the form

$$\hat{H} = \hat{H}_0 + \lambda\hat{H}_1, \quad (6)$$

it has been proven that [11]

$$G^{-1/2} \geq \frac{1}{t\|\hat{H}_1\|}. \quad (7)$$

Above, t is the time of the evolution and $\|\hat{H}_1\|$ is the norm of the operator coupled to $\delta\lambda$. Most importantly, as the time factor might be experimentally limited, the focus usually is on the scaling of the norm only. The above bound holds for any initial state. Saturating it, if at all possible in the general case (even only in the limit of short times), usually requires considering highly entangled Greenberger-Horne-Zeilinger (GHZ)-like probe states.

When the Hamiltonian $\hat{H}_1$ above includes k-body terms, the possible scaling shifts to $G^{-1/2} \sim N^{-k}$ [11], provided that all possible k-body subsets are present in $\hat{H}_1$ to contribute to the norm in Eq. (7). In principle, this might allow one to go beyond the Heisenberg limit for $k \geq 2$. Such democratic couplings are, however, difficult to create in nature. Recently, those results were extended to describe both open and noisy systems [18–22].

The rotation scenario serves also as a powerful entanglement detector [23,24] that can detect a vanishing fraction of entanglement [25] or even bound entanglement [26] with scaling close to the Heisenberg limit. The entanglement detection method has recently found a new application in the proposal to extract the Fisher information from a dynamical susceptibility of the thermal input state [27] (see also Ref. [28]), which is measurable, for instance, by means of Bragg spectroscopy [29,30]. Recently, the pure state metrology in the spirit of the rotation scenario has been reformulated in terms of the Loschmidt echo [31,32]. Let us also mention that one can consider Fisher information as a detector of nonequilibrium phase transitions [33,34] or for multipartite entanglement questions [35]. For a review of quantum enhanced measurements without entanglement, see Ref. [36].

Having all the above in mind, one immediately recalls the second approach that connects the estimation problem to the concept of criticality [37–45]. In that approach one focuses on the situation where the dependence of the state on λ has a completely different origin. The state $|\Psi(\lambda)\rangle$ is the ground state of the Hamiltonian depending on the parameter λ, which exhibits criticality at some critical point λ_c. The essence of this approach is an observation that in the vicinity of the critical point the ground state becomes drastically sensitive to a small change of λ. Clearly, this sensitivity is again quantified by QFI.

In the context of ground-state fidelity (or more generally for the thermal states), it is customary to introduce fidelity susceptibility $\chi_F(\lambda)$. For sufficiently small δ_λ, in a finite system, one has

$$\mathcal{F}[\hat{\rho}(\lambda), \hat{\rho}(\lambda+\delta_\lambda)] = 1 - \frac{1}{2}\chi_F(\lambda)\delta_\lambda^2 + O(\delta_\lambda^3). \quad (8)$$

Fidelity susceptibility and QFI are directly proportional to the Bures distance between density matrices at slightly differing values of λ [40,46] and $G(\lambda) = 4\chi_F(\lambda)$.

Interestingly, it has been observed in this case that for Hamiltonian Eq. (6), criticality can boost QFI to $G^{-1/2} \sim N^{-l}$ with $2 < l < 3$, see Refs. [47–49], leading to an apparent super-Heisenberg scaling. There seems to exist a clear contradiction with the rotation scenario. Can these two pictures be reconciled? This is the main aim of the present work—we solve this super-Heisenberg puzzle. We show that the overlap measurement contains an additional ingredient, namely, the time it takes to transform one ground state into another one at a slightly different parameter value. This may be translated into the additional N-power scaling of time in the vicinity of the critical point if one assumes adiabatic dynamics, which is a necessity if we are to compare ground states. This allows us to reconcile the two approaches to quantum metrology.

The rest of the article is organized as follows. In Sec. II, we define and discuss basic properties of fidelity and fidelity susceptibility, the main tools of the analysis that follow. Section III contains the main results of our work. Using a finite-size scaling hypothesis based on the renormalization group approach, a well-established tool in the treatment of quantum criticality, we derive the scaling of precision offered by the most natural observables coupled to the perturbation. In the adiabatic limit they can saturate the ultimate scaling set by QFI. Most importantly, we also bring the time directly into the picture and discuss the appropriate timescale necessary to recover the adiabatic dynamics at the critical point and reach the above-mentioned scalings. By factoring out the evolution time we illustrate that the ground-state approach naturally satisfies the Heisenberg limit as it is understood in the rotational scenario. The apparent super-Heisenberg scalings are recovered in the limit of sufficiently long evolution times and can be understood as the ultimate limit of precision that can be obtained within this approach (whatever the time is). Using a critical ground state as a probe state, nevertheless, might allow one to break the shot-noise limit due to strong correlations or entanglement in such a state.

The general theory is illustrated on a particular example in Sec. IV. We discuss the ferromagnetic Heisenberg spin chain where the parameter to be estimated is a small external magnetic field. This model provides a minimal entanglement model in a sense that H_1 is separable while H_0 involves only two-body (nearest-neighbors) terms. Here we test the universal scaling of the error propagation formula for those natural observables against numerical data in the immediate vicinity of the critical point of the model. In particular, we obtain in this model $G^{-1/2}(\lambda_c) \sim N^{-1.75}$, with λ_c being the parameter value at the critical point. Moreover, unlike in the standard, rotation-based metrology, the most natural, strictly local, and parameter-independent estimator, namely the single-site magnetization, is enough to go beyond the apparent Heisenberg limit by reaching $N^{-1.5}$. We also show that the operator which measures the magnetization on all sites simultaneously scales in the same way as the optimal one. We should point out that finding an analytical form of the optimal operator in a many-body system is typically a daunting challenge; see, e.g., Refs. [39,40]. With all these interesting properties, when a time factor is properly taken into account (i.e., the time needed to adiabatically transfer a ground state into another ground state at different value of the parameter) we recover the Heisenberg limit.

The possible realization of this model in a cold-atom optical lattice setting is given in Sec. VII. We find it appropriate to first extend the discussion from smooth adiabatic quench to the instantaneous one, i.e., the Loschmidt echo, arguing that similar universal behavior can be observed also in that case. This is discussed in Sec. V. In Sec. VI, we consider the robustness of the observed features; i.e., we consider the situation detuned from criticality as well as the impact of finite temperature. We conclude in Sec. VIII. Finally, in the Appendix, we discuss a universal estimator-type measurement in the paradigm where the original reference state and the specific quadratic interactions are accessible.

II. BASICS OF FIDELITY SUSCEPTIBILITY

Consider the quantum system depending on a parameter λ, the value of which we shall try to estimate. For the ground state $|\Psi(\lambda)\rangle$ of the Hamiltonian $\hat{H}(\lambda)$ the fidelity defined in Eq. (1) simplifies as

$$\mathcal{F} = |\langle\Psi(\lambda)|\Psi(\lambda+\delta_\lambda)\rangle|. \quad (9)$$

It is intuitively clear that fidelity may be significantly below unity, or alternatively that $\chi_F(\lambda)$ [compare Eq. (8)] is large, when the properties of the system change significantly with λ. Then the measurement of some observable might lead to an accurate determination of λ. Clearly, when the system undergoes the quantum phase transition its properties change dramatically; that is why the maxima of $\chi_F(\lambda)$ (for a finite system) or its divergences (in the thermodynamic limit) signal the location of the quantum critical point [37]. Obviously, for Eq. (8) to hold we have to consider a finite system and sufficiently small δ_λ—otherwise higher terms in that expansion are non-negligible

and one should be considering $\log \mathcal{F}$, which becomes an extensive quantity in that limit [50,51].

It has been shown that the universal information can be extracted from the behavior of fidelity susceptibility in the vicinity of the critical point [52–55]. To that end, and in order to relate directly to the rotational scenario in Eqs. (5)–(7), we consider the Hamiltonian

$$\hat{H}(\lambda) = \hat{H}_0 + \lambda \hat{H}_1 = \hat{H}_0 + \lambda \sum_n \hat{h}_n, \tag{10}$$

specifying it to be in a broad class of systems consisting of $N = L^d$ spins in d spatial dimensions which has a continuous critical point at λ_c. The general concept and scaling analysis [56–58] naturally applies also to systems of fermions and bosons. The perturbation coupled to λ in Eq. (10) consists of local on-site terms; note, however, that the same would hold for $\hat{h}_n$ having support on a couple of neighboring sites. $\hat{H}_1$ is a relevant renormalization group perturbation which drives the transition and we assume that it has a well-defined scaling dimension. The divergence of the correlation length in the vicinity of the critical point, $\xi \sim |\lambda - \lambda_c|^{-\nu}$, specifies the critical exponent ν.

The universal part of the fidelity susceptibility at the critical point is expected to scale as [53–55]

$$G(\lambda_c)^{1/2} \sim \chi_F(\lambda_c)^{1/2} \sim N^{1/d\nu}. \tag{11}$$

One may also look at $\chi_F(\lambda)$ away from the critical point where the expected scaling reads

$$G(\lambda)^{1/2} \sim \chi_F(\lambda)^{1/2} \sim N^{1/2} |\lambda - \lambda_c|^{d\nu/2-1}. \tag{12}$$

The above universal contributions dominate the behavior of fidelity susceptibility when $d\nu < 2$, so that nonuniversal, system-specific corrections remain subleading [55,59].

As a consequence, a realization of a physical system with small ν can lead to a hypersensitive estimation of λ. The standard and often considered exactly solvable one-dimensional spin Ising chain where λ corresponds to the transverse field exhibits the critical point with $\nu = 1$, resulting in $\chi_F(\lambda_c)^{1/2} \sim N$ [40,60,61]. In the following we propose a physical realization of another spin system leading to a much smaller value of $d\nu < 1$. This provides a more intriguing example of a system which exhibits extreme sensitivity when λ is varied across the critical point, and, at first sight, might seem to break the Heisenberg limit.

III. METROLOGY AT THE CRITICAL POINT

In this section, we employ the adiabatic theorem to argue how slowly the parameter λ has to change for the system to be able to adjust to it and follow the instantaneous ground state. At the critical point this results in a time factor which scales as a power law with the system size. More generally, we show that the time dependence of QFI satisfies the bound where the time factorizes and the remaining scaling with N can exceed the shot-noise limit due to strong correlations in the critical ground state. It is, however, consistent with the Heisenberg limit in Eq. (7). As such, we reconcile this approach with the rotational scenario. On the other hand, using finite-size scaling analysis we argue that in the adiabatic regime the most natural observables, corresponding to part of the Hamiltonian coupled to λ, offer the same scaling of the error propagation formula as promised by the QFI.

A. Characteristic timescale

First, we estimate the rate of changes of λ which is needed for the system to stay in the instantaneous ground state. We assume that

$$\delta_\lambda(t') = t'/\tau_Q = \frac{t'}{t}\delta_\lambda, \tag{13}$$

for $t' \in [0, t]$, where t is the total time of the evolution, $\delta_\lambda(t) = \delta_\lambda$, and $\tau_Q = t/\delta_\lambda$ is the quench rate. In order to estimate this rate we have to know the behavior of the energy gap at the critical point. For a continuous critical point this gap is expected to scale as $\Delta E \sim L^{-z}$, which introduces the critical exponent z. We also need to estimate the width of the region of λ's for which the gap is close to its minimal value. The standard finite-size argument gives $\Gamma \sim L^{-1/\nu}$. It follows from the general heuristics that in the finite system the gap would be comparable with its minimum when $L \sim \xi(\lambda) \sim |\lambda - \lambda_c|^{-\nu} = \Gamma^{-\nu}$. Now, the adiabatic condition reads $\Gamma \Delta E \gg 1/\tau_Q$; see, e.g., Ref. [62]. This is equivalent to

$$\tau_Q \gg L^{(z\nu+1)/\nu} = N^{(z\nu+1)/d\nu}. \tag{14}$$

The same estimate of the relevant quench rate is obtained from the application of the Kibble-Zurek argument [63–65]. The latter predicts the density of defects excited during the slow quench across the critical point. The adiabatic dynamics corresponds, in that case, to the extreme limit when no defects are created in a finite system.

In order to induce the change of the parameter $\delta_\lambda \sim N^{-1/d\nu}$ which, according to Eq. (11), can possibly be observed, the time must scale at least as

$$\hat{t} \sim \tau_Q \delta_\lambda \sim N^{z/d}. \tag{15}$$

Otherwise, Eq. (15) simply represents the characteristic timescale at the critical point, given by the inverse of the energy gap in the finite system. This means that this timescale would naturally be relevant also beyond the scheme assuming adiabatic evolution and the ground-state overlap. We further elaborate on this point in Sec. V, where we briefly discuss how a small instantaneous quench and

Loschmidt echo naturally fits into the general picture discussed here.

We can now bring those scalings together. The bound in Eq. (7) applied to the ground-state fidelity scenario would then read

$$N^{-1/d\nu} \sim G(\lambda_c)^{-1/2} \geq 1/\hat{t}\|\hat{H}_1\| \sim N^{-z/d-1}; \quad (16)$$

note that $\|\hat{H}_1\| \sim N$, which corresponds to the usual Heisenberg factor. In this reasoning we make a straightforward generalization of the argument of Ref. [11], valid for time-independent systems, to the time-dependent adiabatic evolution. In the scaling sense, Eq. (16) is equivalent to the condition that $(z+d)\nu \geq 1$.

At this point it is convenient to introduce the scaling dimension of the operator $\hat{h}$, $[h]$, which describes the rescaling of the operator upon the scale transformation at the critical point. It gives the power-law behavior of the connected correlation function $C(r) = \langle \hat{h}_n \hat{h}_{n+r}\rangle - \langle \hat{h}_n\rangle\langle \hat{h}_{n+r}\rangle \sim r^{-2[h]}$ in the thermodynamic limit. The scaling exponents are not independent but, as we have one relevant operator here, can be typically expressed as a combination of $[h]$, z, and d. For instance, $\nu = 1/(d+z-[h])$ [58,66]. As $[h] \geq 0$, this shows that Eq. (16) is indeed consistent within our scaling discussion as $(z+d)\nu \geq 1$ holds.

B. Error propagation formula in the adiabatic limit

Second, we focus on the adiabatic limit, where we discuss the scaling of the error propagation formula of the most natural observables $\hat{H}_1$ and $\hat{h} = \hat{h}_{N/2}$. We assume $\hat{h}$ to be in the bulk of the system to avoid possible effects related with the boundaries of the system. It is an exercise in finite-size scaling analysis to argue that at the critical point

$$\Delta_{\delta_\lambda}(\hat{H}_1, \lambda_c) \sim N^{-1/d\nu}, \quad (17)$$

$$\Delta_{\delta_\lambda}(\hat{h}_{N/2}, \lambda_c) \sim N^{-1/d\nu+[h]/d}. \quad (18)$$

The Eq. (17) is saturating the bound provided by the fidelity susceptibility and Eq. (18) is close to it for small $[h]$; see below for the derivation under the assumption that in a d-dimensional system the correlation function is vanishing with distance r slower than r^{-d}, and that the hyperscaling relations hold. Those scalings are closely connected with the important observation that fidelity susceptibility (QFI) can be directly calculated by integrating the dynamic susceptibility of the system to the external driving $\hat{H}_1$ [27,52–54,67].

In order to derive Eqs. (17) and (18) we analyze the scaling of the standard deviation and susceptibility appearing in the error propagation formula in Eq. (3). In the thermodynamic limit, the susceptibility $\partial_\lambda\langle\hat{h}\rangle \sim |\lambda-\lambda_c|^{-\theta}$. We assume that the hyperscaling law holds, i.e., that there are no dangerous irrelevant operators which could modify the scaling hypothesis. In that case, $\theta = 1-[h]\nu$. It is expected to hold for a sufficiently low-dimensional system, not exceeding the so-called upper critical dimension. This is the limit of interest from the perspective of quantum enhanced metrology, as the quantum effects in quantum many-body systems are becoming less important with the growing dimension of the system due to the monogamy of entanglement. In the above, we also assume that $\theta \geq 0$. Otherwise, nonuniversal effects dominate the behavior of susceptibility, and effectively $\theta = 0$. Now, the standard finite-size scaling argument implies that for a finite system at the critical point $\partial_\lambda\langle\hat{h}\rangle \sim (L^{-1/\nu})^{-\theta} \sim N^{\theta/d\nu}$. Assuming that the standard deviation s.d.$(\hat{h}) \sim 1$ leads to Eq. (18), where we have used the hyperscaling relation.

Similarly, the susceptibility $\partial_\lambda\langle\hat{H}_1\rangle \sim N^{1+\theta/d\nu}$ follows from the scaling for $\hat{h}$ (times factor of N; we additionally assume that possible boundary effects are subleading). It is then enough to estimate the behavior of the standard deviation where we have to take into account the correlator $C(r) \sim r^{-2[h]}$ in the ground state at the critical point. The leading behavior is obtained by integrating the correlation function over the d-dimensional ball of radius L. If $C(r)$ is not vanishing faster than r^{-d}, i.e., for $d-2[h] > 0$, the integral is dominated by the tail of the correlation function and gives $\sqrt{\langle\hat{H}_1^2\rangle - \langle\hat{H}_1\rangle^2} \sim L^{d-[h]} = N^{1-[h]/d}$. Note that the standard deviation corresponds to a structure factor at $k = 0$. Combining the expected scaling of standard deviation and susceptibility together with the hyperscaling relation gives Eq. (17).

It is worth discussing the case of $d-2[h] \leq 0$ as well. Here, $\sqrt{\langle\hat{H}_1^2\rangle - \langle\hat{H}_1\rangle^2} \sim L^{d/2} = N^{1/2}$ and, consequently, $\Delta_{\delta_\lambda}(\hat{H}_1, \lambda_c) \sim N^{-1/d\nu+[h]/d-1/2}$. It does not saturate the bound given by QFI and we only see the classical $N^{-1/2}$ improvement over the single-site measurement in Eq. (18). This is, for instance, the case in the often discussed quantum Ising spin chain in the transverse field, $\hat{H} = -\sum_{n=1}^{N}\sigma_n^x\sigma_{n+1}^x + g\sigma_n^z$. It has a critical point for $g_c = 1$ with the exponent $z = 1$. When $\hat{h}_n = \sigma_n^z$ corresponds to the transverse field, the scaling dimension $[h] = 1$, $\nu = 1$, and effectively $\theta = 0$. The error propagation formula for $\hat{H}_1 = \sum_n\sigma_n^z$ was calculated in Ref. [43] and does not saturate the scaling of $G^{-1/2}(g_c) \sim N$. It reads $\Delta_{\delta_\lambda}(\hat{H}_1, \lambda_c) \sim [N\log(N)]^{-1/2}$, in agreement with the general prediction above. We note that logarithmic corrections to the scaling are typically expected in this case as $\theta = 0$.

C. Consistency with the rotational scenario

The above scalings of the error propagation formula assume adiabatic dynamics and as such would be recovered for long enough evolution times. At this point, we bring the time explicitly into the picture. We show that

$$G(\lambda,t)^{1/2} \leq t2\zeta\sqrt{\langle\hat{H}_1^2\rangle - \langle\hat{H}_1\rangle^2}, \tag{19}$$

where the standard deviation is calculated in the initial ground state. The factor $\zeta = (1/t\delta_\lambda)\int_0^t dt'\delta_\lambda(t')$ follows from the evolution profile in Eq. (13). Here, $\zeta = 1/2$. Equation (19) represents the quantum speed limit adjusted to our setting. For a recent review on quantum speed limits, see, e.g., Ref. [68].

For a system at the critical point, as discussed in the previous section, this leads to

$$G(\lambda_c,t)^{1/2} \lesssim t2\zeta N^{1-[h]/d}. \tag{20}$$

We assume here that the correlations $C(r) \sim r^{-2[h]}$ do not vanish to quickly and $d > 2[h]$. Obviously, as $[h] \geq 0$, Eq. (20) is within the general bound (valid for any initial state) given by the Heisenberg limit. In this article—and more generally in the ground-state fidelity approach—the focus is on the ground state of the critical system and the evolution generated by the Hamiltonian slightly perturbed from it. As can be seen in Eq. (20), this allows one to go beyond the shot-noise limit, $G(\lambda,t) \sim tN^{1/2}$, as a result of strong entanglement of such an initial state and algebraically vanishing $C(r)$.

For the system detuned from criticality, or when $d - 2[h] \leq 0$, the variance in Eq. (19) is not superextensive and the classical scaling with N is recovered. This would again be the case for the Ising model briefly discussed at the end of the previous section. There, for $\hat{h}_n = \sigma_n^z$ corresponding to the transverse direction, $C(r) \sim r^{-2}$ at the critical point.

It is worth comparing this with the rotational scenario, in which case the suitable GHZ-type probe state is usually considered. We would then have $C(r) \sim 1$ and effectively $[h] = 0$, which saturate the scaling of the Heisenberg limit (at least for short times). Interestingly, a critical spin Hamiltonian for which the GHZ state is the ground state can be supplied [69,70].

The scalings in Eqs. (11), (17), and (18) are reached for the evolution times of the order of $\hat{t} \sim N^{z/d}$, Eq. (15). They comprise the ultimate limits of the criticality-based quantum metrology, giving the title of this article a proper meaning.

To derive Eq. (19) we straightforwardly generalized the result of Refs. [13–15] to the time-dependent Hamiltonian, with $\delta_\lambda(t')$, e.g., as in Eq. (13). This leads to [71]

$$G(\lambda,t) = 4\zeta^2t^2(\langle\Psi|\hat{O}_1^2|\Psi\rangle - \langle\Psi|\hat{O}_1|\Psi\rangle^2) = 4\zeta^2t^2\mathrm{var}(\hat{O}_1),$$

where $\hat{O}_1 = (1/t\delta_\lambda\zeta)\int_0^t dt'\delta_\lambda(t')U(\lambda,t-t')^\dagger\hat{H}_1U(\lambda,t-t')$ is the time-averaged operator $\hat{H}_1$ rotated by $U(\lambda,t) = e^{-it\hat{H}(\lambda)}$ and $|\Psi\rangle$ is the probe state. As variance is convex, we have $G(\lambda,t) \leq 4t^2\zeta^2(1/t\delta_\lambda\zeta)\int_0^t dt'\delta_\lambda(t')\times \mathrm{var}[U(\lambda,t-t')^\dagger\hat{H}_1U(\lambda,t-t')]$. In our setup we consider the initial state which is the ground state of $\hat{H}(\lambda)$, $|\Psi\rangle = |\Psi(\lambda)\rangle$, which leads to Eq. (19).

IV. EXAMPLE: *XXZ* MODEL IN THE EXTERNAL FIELD

The discussion in the previous section is general and should hold for a broad class of systems exhibiting continuous quantum critical points. In order to illustrate those predictions, in this section we consider the ferromagnetic XXZ spin-1/2 spin chain in the external field. The Hamiltonian reads

$$\hat{H}(\lambda) = -\sum_{n=1}^{N-1}(\sigma_n^x\sigma_{n+1}^x + \sigma_n^y\sigma_{n+1}^y + J_z\sigma_n^z\sigma_{n+1}^z) + \lambda\sum_{n=1}^{N}\sigma_n^x, \tag{21}$$

where we assume open boundary conditions. $N = L$ is the number of spins ($d = 1$) and J_z is an anisotropy parameter. We consider changes induced by the magnetic field λ with other parameters fixed. For $|J_z| \leq 1$, the system has a critical point at $\lambda_c = 0$ with the critical exponent $z = 1$. The exponent ν was calculated in Ref. [72] and for fixed $-1 < J_z < 1$ reads

$$\nu = \frac{2}{4 - \arccos(J_z)/\pi}, \tag{22}$$

which follows from the scaling dimension of the operator σ^x, $[\sigma^x] = \arccos(J_z)/2\pi$. The desired condition of $d\nu < 1$ is satisfied for all values of $|J_z| < 1$.

We note that fidelity susceptibility for a quite similar XXZ model was studied, e.g., in Refs. [73–75] at both zero and nonzero temperature. There, however, the external magnetic field λ was not present and the shift of parameters was induced by changing the value of J_z. This leads to a qualitatively different type of behavior related with the Berezinskii-Kosterlitz-Thouless critical point, and in that case the system does not exhibit superextensive scaling of the fidelity susceptibility.

At the risk of multiplying the notation, let us define the following observables:

$$\hat{M}_x \equiv \hat{H}_1 = \sum_{n=1}^{N}\hat{\sigma}_n^x, \tag{23}$$

which corresponds to the simultaneous measurement of magnetization on all sites, and

$$\hat{m}_x \equiv \hat{h}_{N/2} = \hat{\sigma}_{N/2}^x, \tag{24}$$

i.e., the on-site magnetization in the center of the system.

In Fig. 1, we calculate both QFI and the error propagation formula for $\hat{M}_x$ and $\hat{m}_x$ in the adiabatic limit. We

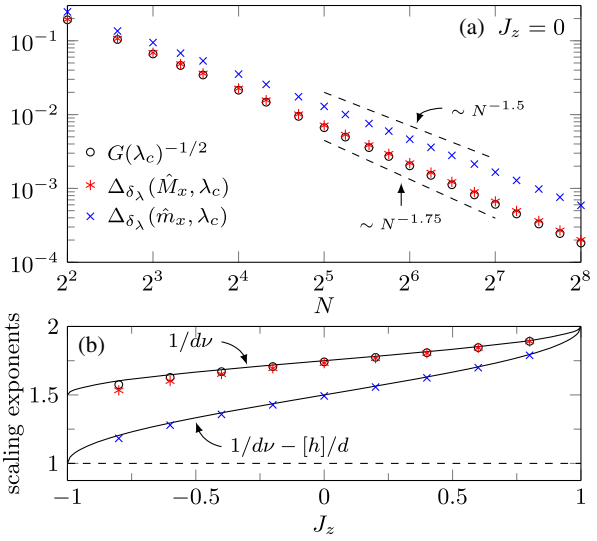

FIG. 1. XXZ model in the external field, Eq. (21). (a) Scaling of the error propagation formula for operators $\hat{M}_x$ and $\hat{m}_x$, and the ultimate bound given by inverse of QFI, as a function of the system size. The error propagation formula for $\hat{M}_x$ closely follows the ultimate bound. Dashed lines indicate the slopes corresponding to the expected scaling and serve as guidance for the eye. The fits give $G(\lambda_c)^{-1/2} \sim N^{-1.74}$, $\Delta_{\delta_\lambda}(\hat{M}_x, \lambda_c) \sim N^{-1.73}$, and $\Delta_{\delta_\lambda}(\hat{m}_x, \lambda_c) \sim N^{-1.49}$, where the expected exponents are 1.75, 1.75, and 1.5, respectively. Here, $J_z = 0$ and the fits were done for $N = 128 - 256$ [76]. (b) In the considered model the scaling exponents in Eqs. (11), (17), and (18) depend continuously on the value of parameter J_z, following Eq. (22). We compare those predictions with numerical results obtained similarly as in (a). The exponent associated with the standard Heisenberg limit is marked with the dashed line for comparison. Its apparent breaking is the main subject of this article.

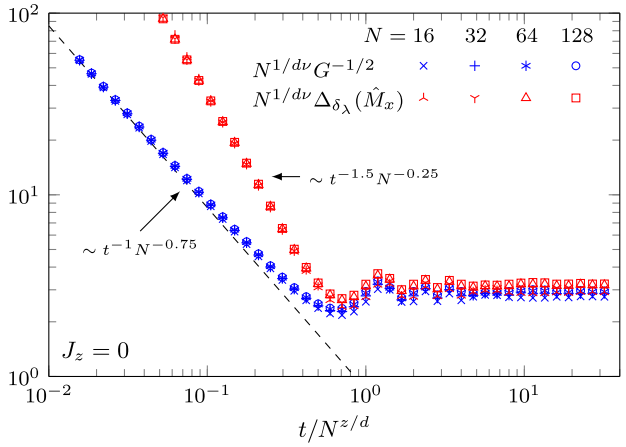

FIG. 2. Time dependence of QFI at the critical point in the XXZ model. Results from a small external magnetic field change as in Eq. (13). The time is rescaled by the system size according to Eq. (15). QFI (blue symbols) is rescaled corresponding to the adiabatic limit given by Eq. (11). Here, for $J_z = 0$, $z/d = 1$ and $d\nu = 4/7$. For evolution times $t \gg N^{z/d}$ we recover the adiabatic limit. For short times $G^{1/2} \sim tN^{1-[h]/d}$, which is marked with dashed line. In our case, $1 - [h]/d = 3/4$. We also show the time dependence of the precision allowed by $\hat{M}_x$, as described by the error propagation formula (red symbols). For long time, in the adiabatic limit, it is almost optimal and nearly saturates QFI. For short times it is suboptimal. In that case $\Delta_{\delta_\lambda}(\hat{M}_x, \lambda_c, t) \sim t^{-1.5}N^{-0.25}$ is below the shot-noise limit as a function of N, see Eq. (25), a result of strong fluctuation at the critical point.

numerically verify that the scaling relations in Eqs. (11), (17), and (18) indeed hold in our model. Most importantly, it can be seen that the very natural operator $\hat{M}_x$ practically reproduces the apparent super-Heisenberg scaling allowed by QFI. Moreover, while on-site magnetization in the bulk, $\hat{m}_x$, grows slower with the system size then the ultimate bound, it is still well in the apparent super-Heisenberg regime. For instance, Eqs. (17), (18), and (22) imply that for $J_z = 0$, we expect $\Delta_{\delta_\lambda}(\hat{M}_x, \lambda_c) \sim N^{-7/4}$ and $\Delta_{\delta_\lambda}(\hat{m}_x, \lambda_c) \sim N^{-3/2}$. This is in excellent agreement with the numerical results presented in Fig. 1(a). The exponents for other values of the parameter J_z, both theoretical predictions and the values fitted from the numerics, are shown in Fig. 1(b).

The above results were obtained assuming that the evolution is adiabatic and the time of the evolution might have been, in principle, infinite. We present the limitations imposed by finite evolution time in Fig. 2. To that end, the system was initialized in the ground state at the critical point $\lambda_c = 0$. Subsequently, it was evolved to some infinitesimal δ_λ according to Eq. (13), with $\tau_Q = t/\delta_\lambda$ set by the total evolution time and δ_λ. We then use Eq. (1) to calculate QFI as a discrete derivative corresponding to Eq. (2) (for small enough δ_λ).

We rescale the evolution time with the characteristic timescale in Eq. (15) and the QFI according to the adiabatic (long-time) limit in Eq. (11). As can be seen in Fig. 2, the rescaled data obtained for different system sizes collapse, corroborating the scaling predictions. QFI saturates at its adiabatic limit at the time given by Eq. (15). We obtain similar collapse for other values of the anisotropy parameter J_z (not shown).

The bound on QFI given by Eq. (19) is plotted with the dashed line. The bound is tight in the limit of short times, in which case $G(\lambda_c, t)^{1/2} \sim tN^{3/4}$ for $J_z = 0$ plotted in Fig. 2. This scaling is obviously in full agreement with the Heisenberg limit. Employing the ground state of the critical system as a probe allows one, however, to go beyond the shot-noise limit.

Finally, in Fig. 2 we show how sensitivity allowed by $\hat{M}_x$ depends on time in our setup. As expected, for long enough times, $\Delta_{\delta_\lambda}(\hat{M}_x, \lambda_c, t)$ saturates at the adiabatic value, almost saturating the ultimate QFI bound. It is, however, far from being optimal for short times. In that case, for $1 \ll t \ll N^{z/d}$ we can expect [77]

$$\Delta_{\delta_\lambda}(\hat{H}_1, \lambda_c, t) \sim t^{-\theta/z\nu}N^{-[h]/d}. \tag{25}$$

For $J_z = 0$ in Fig. 2 this translates into $\Delta_{\delta_\lambda}(\hat{M}_x, \lambda_c, t) \sim t^{-3/2}N^{-1/4}$. Such scaling of an error propagation formula in the limit of short times follows from the behavior of susceptibility, i.e., the denominator in Eq. (3). The susceptibility $\partial_\lambda \langle \hat{H}_1 \rangle \sim N t^{\theta/z\nu}$, which directly follows from the universal scaling of dynamical susceptibility at the critical point [56,57]. As the standard deviation $\sqrt{\langle \hat{H}_1^2 \rangle - \langle \hat{H}_1 \rangle^2} \sim N^{1-[h]/d}$ is set by the reference initial state, this gives Eq. (25). This derivation demonstrates that in this limit strong fluctuations—corresponding to slowly vanishing correlation $C(r)$—limit the precision allowed by the operator $\hat{H}_1$, putting it below the shot-noise limit. Conversely, we would be able to recover the shot-noise limit here for $C(r)$ vanishing faster then r^{-d} (or away from the critical point).

All numerical results presented in this section were obtained using the toolbox of matrix product states (MPS) [78–80]. The time evolution is simulated using the time-dependent variational principle [80], which projects the Schrödinger equation onto the tangent space of the manifold of the MPS. For our problem, we use the fourth-order time-dependent Suzuki-Trotter decomposition [81], necessary to split the unitary evolution operator onto parts acting on matrices of MPS associated with individual spins. We check that the results are converged in both the discreet time step and MPS bond dimension.

The natural question is how to produce or emulate the above physical system. Such a spin model may be possibly realized for repulsively interacting ultracold bosons in optical lattice potential in a quasi-one-dimensional geometry resulting from tight confinement in the perpendicular directions. The optical lattice potential can be precisely controlled, in particular, it can be shaken laterally [82,83], which allows us to change the system properties. By modulating the intensity of the laser beams forming the optical lattice, its depth can also be modulated periodically [84]. Assuming that both processes occur with the same frequency ω, a frequency that is much larger than the tunneling frequency as well as a characteristic frequency due to interactions, one can derive an effective time-averaged Hamiltonian governing the long-time physics, as reviewed, e.g., in Refs. [85–87]. Importantly, we assume that this frequency (or rather its integer multiple, $\mathcal{N}\omega$) is resonant with the $s \to p$ transition between the lowest s and the excited p band. Such a resonance leads to additional slowly varying terms that affect the effective Hamiltonian obtained after time averaging.

Consider such a system with unit mean filling. Identifying the proper ground-state manifold one may describe the dynamics with an effective spin Hamiltonian. Depending on $\mathcal{N}$ one may realize the effective XXZ Heisenberg model for $\mathcal{N} = 2$, or the model that reduces to the desired XXZ Heisenberg Hamiltonian in the magnetic field in Eq. (21) for $\mathcal{N} = 3$. For the interested readers, we provide the explicit derivation in Sec. VII, while we first show that analogical universal behavior holds for instantaneous quench of the Hamiltonian, i.e., the Loschmidt echo. We discuss as well the possible effects due to an imperfect tuning and a finite temperature.

V. LOSCHMIDT ECHO

In the previous sections, in order to be able to recover the limit of adiabatic evolution, we were considering parameter λ changing smoothly in time as in Eq. (13). For completeness of the discussion we briefly comment that qualitatively similar behavior is obtained in the other extreme limit, namely, that of a sudden quench. Such a situation is closer to the original spirit of the rotational scenario where the Hamiltonian generating the evolution is usually time independent. To that end, we are again going to initialize the system in the ground state of the initial Hamiltonian, focusing on the critical point as the most interesting regime, and consider evolution generated by the Hamiltonian detuned by δ_λ. Fidelity in Eq. (1) gives directly the so-called Loschmidt echo, which received significant attention in the literature [88], for instance, in the studies of decoherence. Most notably for us, it was shown that the decay of the Loschmidt echo is enhanced at the vicinity of the quantum critical point [89].

We illustrate the time dependence of the QFI calculated in this setting, $G_{\mathrm{LE}}(\lambda, t)$, for our XXZ model at the critical

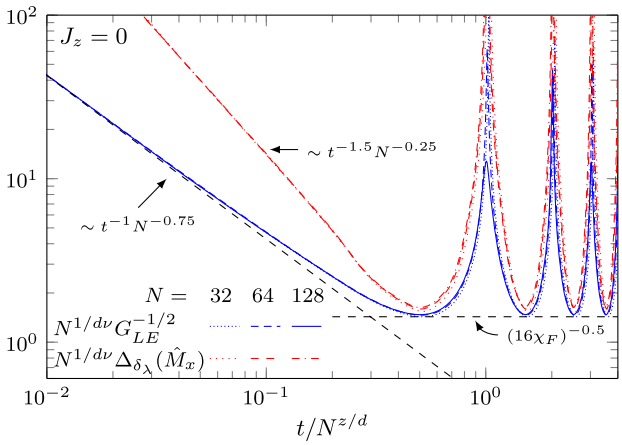

FIG. 3. Time dependence of QFI at the critical point in the XXZ model, which results from a small instantaneous shift of the external magnetic field, i.e., the Loschmidt echo. The time is rescaled by the system size according to Eq. (15). The maximal value which can be reached by QFI is bounded by the ground-state fidelity susceptibility (dashed line). We rescale QFI (blue lines) according to Eq. (11). Here, for $J_z = 0$, $z/d = 1$ and $d\nu = 4/7$. For short times, $G^{1/2} \sim tN^{1-[h]/d}$, marked with dashed line, with $1 - [h]/d = 3/4$ in our case. For evolution time $t \sim N^{z/d}$, QFI almost reaches it maximal value and later exhibits periodic revivals characteristic for the Loschmidt echo. We also show the time dependence of the precision allowed by $\hat{M}_x$ (red lines). For long time it is close to optimal, mimicking the behavior of QFI. For short times it is suboptimal. In that case, $\Delta_{\delta_\lambda}(\hat{M}_x, \lambda_c, t) \sim t^{-1.5}N^{-0.25}$ is below the shot-noise limit as a function of N; see Eq. (25).

point with $J_z = 0$ in Fig. 3. The scaling behavior is similar to the smooth quench shown in Fig. 2. Indeed, the general bound in Eq. (19) directly applies to this case, where now $\delta_\lambda(t') = \delta_\lambda$ and $\zeta = 1$. For very short times the bound is tight [90], which follows from the perturbation theory [91], and at the critical point we again get $G^{1/2}_{\mathrm{LE}}(\lambda_c, t) \sim tN^{1-[h]/d}$ [under the assumption that $C(r)$ is not vanishing too quickly] [92,93]. As we consider evolution of the initial ground state by the Hamiltonian which is slightly detuned from the initial one, it is easy to see that QFI cannot grow unbounded and $G^{1/2}_{\mathrm{LE}}(\lambda, t) \leq 2G^{1/2}(\lambda)$. Here, $G(\lambda) = 4\chi_F(\lambda)$ corresponds to ground-state fidelity. At the critical point the bound is reached at the timescale given by Eq. (15). In opposition to the smooth (adiabatic) scenario, Loschmidt echo displays revivals visible as peaks in Fig. 3, characteristic for the critical point [88]. The operator $\hat{M}_x \equiv \hat{H}_1$ again proves to offer a near optimal precision for long times. For short times the derivations in the previous section and Eq. (25) are expected to similarly hold, as can indeed be seen in Fig. 3.

VI. ROBUSTNESS TO DETUNING FROM CRITICALITY

To complete the study of scaling results for the error propagation formula, it is quite natural to ask to what extent such a scaling is relevant in real systems, for example, due to a nonperfect tuning to the phase transition point and/or a finite temperature of an experiment. Fortunately, general scaling predictions addressing this issue can be provided and verified by numerical simulations, which we show in this section.

First, when λ is not tuned sufficiently close to the critical point, the fidelity susceptibility depends linearly on N as discussed around Eq. (12). The crossover is expected for $L/\xi \sim L|\lambda - \lambda_c|^\nu \sim 1$, where ξ is the correlation length. This means that in order to obtain an apparent super-Heisenberg scaling, λ should be tuned to the critical point within $|\lambda - \lambda_c| \ll L^{-1/\nu}$. This is also the range of δ_λ which can be observed in this case.

In the opposite limit of $|\lambda - \lambda_c| \gg L^{-1/\nu}$, away from the critical point, the error propagation formulas are expected to scale as

$$\Delta_{\delta_\lambda}(\hat{H}_1, \lambda) \sim N^{-1/2}|\lambda - \lambda_c|^{1-d\nu/2}, \tag{26}$$

$$\Delta_{\delta_\lambda}(\hat{h}, \lambda) \sim N^{0}|\lambda - \lambda_c|^{-\theta}. \tag{27}$$

The derivation is analogical as in Sec. III. The susceptibility $\partial_\lambda\langle\hat{h}\rangle \sim |\lambda - \lambda_c|^{-\theta}$, together with $\mathrm{s.d.}(\hat{h}) \sim 1$, trivially gives the second of the above relations. For the first one, the standard scaling argument estimates the standard deviation (or a static structure factor) as $\sqrt{\langle\hat{H}_1^2\rangle - \langle\hat{H}_1\rangle^2} \sim N^{1/2}\xi^{d/2-[h]} \sim N^{1/2}|\lambda - \lambda_c|^{-\nu d/2+\nu[h]}$, where the correlations are approximately algebraic $\sim r^{-2[h]}$ up to a distance given by the correlation length ξ. Similarly as in Sec. III, we assume here that the algebraic part of the correlation function is vanishing slower then r^{-d}. Otherwise, long-distance behavior contributes subleadingly to the standard deviation. Finally, combining this with the susceptibility $\partial_\lambda\langle\hat{H}_1\rangle \sim N|\lambda - \lambda_c|^{-\theta}$, together with the hyperscaling relation for θ, gives Eq. (26).

In Fig. 4, we numerically verify those scaling predictions for $J_z = 0$ in the XXZ model in Eq. (21). While away from the critical point the accuracy allowed by $m_x \equiv \hat{h} = \sigma^x_{N/2}$ becomes significantly worse then the optimal one, the accuracy of $\hat{M}_x \equiv \hat{H}_1 = \sum_n \sigma^x_n$ closely follows the ultimate bound set by QFI. It is worth pointing out that even though we have classical $N^{-1/2}$ scaling in this limit, being in the vicinity of the critical point significantly improves the prefactor as, in general, for $d\nu < 2$, $|\lambda - \lambda_c|^{1-d\nu/2} \ll 1$. Similarly as discussed in the previous sections for the critical point, this enhancement comes at a price of suitably longer evolution times. Here, however, the characteristic timescale $\hat{t} \sim \xi^z \sim |\lambda - \lambda_c|^{-z\nu}$ is independent of N.

Second, the pure state idealization discussed so far cannot be fully realized due to the external noise, including the thermal one. Here, for simplicity, we consider the situation where the temperature T is finite but $\lambda = \lambda_c$ is exactly tuned to the critical point. As the finite-size energy

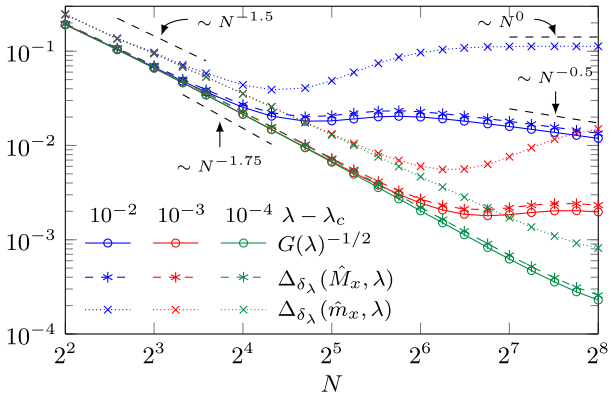

FIG. 4. The crossover between different scaling limits when λ is not tuned exactly to the critical point. Results correspond to the adiabatic limit of the evolution. For given deviation $\lambda - \lambda_c$ we recover the apparent super-Heisenberg scaling when N is small enough. When the system size is further increased and $N/\xi^d \sim N|\lambda - \lambda_c|^{d\nu} \gg 1$, $G(\lambda)^{-1/2}$ and $\Delta_{\delta_\lambda}(\hat{M}_x, \lambda)$ have a crossover to the classical $N^{-1/2}$ dependence. On the other hand, $\Delta_{\delta_\lambda}(\hat{m}_x, \lambda)$ saturates and becomes xindependent on the system size in that limit. Nevertheless, notice that even in this case the prefactors in front of $N^{-1/2(0)}$ are enhanced by the vicinity of the critical point. $\Delta_{\delta_\lambda}(\hat{M}_x, \lambda)$ is closely following the optimal bound set by QFI for all values of the parameters. Dashed lines indicate various scalings and serve as guidance for the eye. Results for the XXZ model in the external field in Eq. (21) with $J_z = 0$.

gap at the critical point scales as L^{-z}, one expects an apparent super-Heisenberg behavior to hold for $T \ll L^{-z}$.

In the opposite limit of $T \gg L^{-z}$ we recover the classical behavior. We expect

$$\Delta_{\delta_\lambda}(\hat{H}_1, \lambda_c, T) \sim N^{-1/2} T^{(1-d\nu/2)/z\nu}, \tag{28}$$

$$\Delta_{\delta_\lambda}(\hat{h}, \lambda_c, T) \sim N^0 T^{-\theta/z\nu}. \tag{29}$$

To that end, in order to simplify the analysis, we assume that there is no line of thermal phase transitions terminating at the quantum critical point which could alter the behavior and we employ simple scaling analysis; see, e.g., Ref. [58]. This is the case for our exemplary XXZ model and, more broadly, for one-dimensional systems.

In this case, the susceptibility $\partial_\lambda \langle \hat{h} \rangle \sim T^{-\theta/z\nu}$ leads to the second of the above relations. With the correlation length $\xi_T \sim T^{-1/z}$, the estimation of the standard deviation gives $\sqrt{\langle \hat{H}_1^2 \rangle - \langle \hat{H}_1 \rangle^2} \sim N^{1/2} \xi_T^{-d/2+[h]} \sim N^{1/2} T^{-d/2z+[h]/z}$, where we again assume that the algebraic part of the correlation function is vanishing slower than r^{-d}. Similarly as in the previous case, $\partial_\lambda \langle \hat{H}_1 \rangle \sim N T^{-\theta/z\nu}$, together with the hyperscaling relation, results in Eq. (28).

We illustrate those scaling predictions in our model for $J_z = 0$ in Fig. 5. We employ MPS calculations, where the finite-temperature density matrix $\hat{\rho}(\lambda) \sim e^{-\hat{H}(\lambda)/T}$ is expressed as purification and obtained via simulation of the finite system in the imaginary time [78–80]. We again employ a time-dependent variational principle to that end.

Direct computation of fidelity in Eq. (1) and, in particular, finding the positive square root appearing there is not feasible in the MPS representation. We then follow Ref. [74], and in this case calculate the fidelity defined as $\tilde{F}[\hat{\rho}(\lambda), \hat{\rho}(\lambda+\delta_\lambda)] = \sqrt{\mathrm{Tr}[\hat{\rho}(\lambda)^{1/2} \hat{\rho}(\lambda+\delta_\lambda)^{1/2}]}$. Importantly, as discussed in Ref. [74] and derived in Ref. [54], if one uses this definition to calculate fidelity susceptibility $\tilde{\chi}_F(\lambda)$ [similarly as in Eq. (8)], then $\tilde{\chi}_F(\lambda) \leq \chi_F(\lambda) \leq 2\tilde{\chi}_F(\lambda)$. This allows us to define $\tilde{G}(\lambda, T) = 8\tilde{\chi}_F(\lambda)$, which sets an upper bound on Fisher information, $\tilde{G}(\lambda, T)/2 < G(\lambda, T) < \tilde{G}(\lambda, T)$, and which we plot in Fig. 5. Those bounds cannot be tightened. Exact diagonalization done for systems of few spins suggests that $G(\lambda, T) \approx \tilde{G}(\lambda, T)/2$ in the limit of small enough N or T. This is also seen in Fig. 5 from comparison to the data for $T = 0$. In the opposite limit of large enough N or T, $G(\lambda, T) \approx \tilde{G}(\lambda, T)$.

In our exemplary XXZ model, $z = 1$. Therefore, for $J_z = 0$ and for a large enough system size or temperature, we expect the scalings $\Delta_{\delta_\lambda}(\hat{H}_1, \lambda_c, T) \sim N^{-1/2} T^{1.25}$ and $\Delta_{\delta_\lambda}(\hat{h}, \lambda_c, T) \sim N^0 T^{1.5}$, which follow from Eqs. (28) and (29). By fitting the temperature dependence to the numerical results for $N = 2^6$, i.e., the largest size in Fig. 5, and $T = 0.25 - 1$, we obtain the exponents equal to 1.2 and 1.55, respectively. This is in reasonable agreement with the scaling predictions, especially given the numerical limitations. Simulations of the thermal states with MPS is typically much more demanding than the case of pure states, especially in the critical systems, which limits the system sizes that can be simulated here.

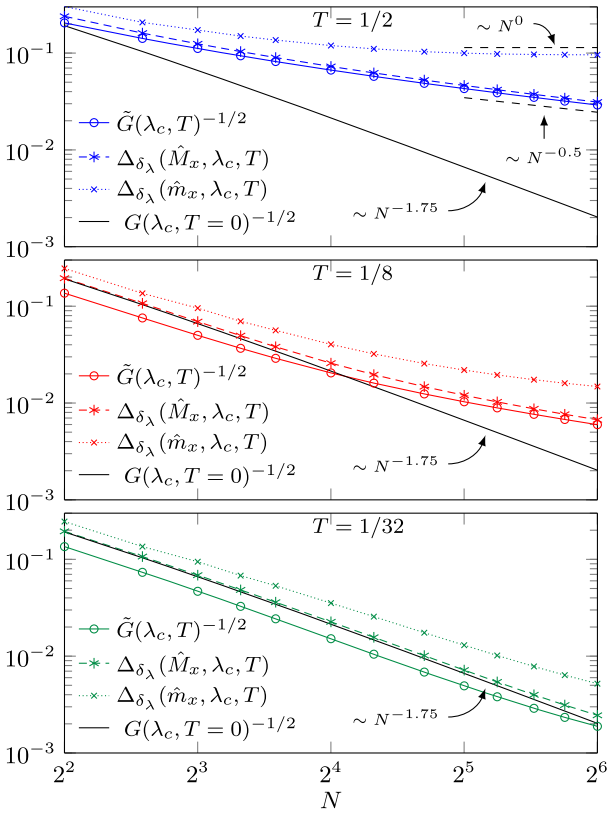

FIG. 5. The crossover between different scaling limits when the temperature T is nonzero. Results obtained by comparing states at equilibrium. For given small T we recover the apparent super-Heisenberg scaling when N is small enough, or alternatively, for $T \ll N^{-z/d}$. In the opposite limit, when the system size is further increased and $NT^{d/z} \gg 1$, $\tilde{G}(\lambda_c, T)^{-1/2}$ and $\Delta_{\delta_\lambda}(\hat{M}_x, \lambda_c, T)$ have a crossover to the classical $N^{-1/2}$ dependence, however, with the prefactors that are enhanced by the presence of a quantum critical point at $T = 0$. $\Delta_{\delta_\lambda}(\hat{m}_x, \lambda, T)$ saturates and becomes independent on the system size in that limit. Similarly as in Fig. 4, we observe that $\Delta_{\delta_\lambda}(\hat{H}_1, \lambda, T)$ is closely following the optimal bound set by QFI even at nonzero temperatures. $\tilde{G}(\lambda_c, T)^{-1/2}$ plotted here is a lower bound of the (inverse of the square root of) Fisher information, which lies between $\tilde{G}(\lambda_c, T)^{-1/2}$ and $(\tilde{G}(\lambda_c, T)/2)^{-1/2}$; see text for discussion. Solid lines show the corresponding ultimate bound for $T = 0$ from Fig. 1. Dashed lines indicate various scalings and serve as guidance for the eye. Results for $J_z = 0$.

It is also worth pointing out that, as can be seen in Fig. 5, $\Delta_{\delta_\lambda}(\hat{H}_1, \lambda_c, T)$ is again closely following the optimal bound set by an inverse of the Fisher information. This is consistent with the scaling of QFI which, similarly to Eqs. (11) and (12), can be deduced from the scaling

dimension of the fidelity susceptibility [52,53] and standard scaling argument. Those give $\chi_F(\lambda_c, T) \sim NT^{(d\nu-2)/z\nu}$.

At the risk of stating the obvious, it is worth pointing out that the scaling predictions in Eqs. (17) and (18) and in Eqs. (28) and (29) correspond to a different order of taking the limits of $T \to 0$ and $N \to \infty$ with the smooth crossover when the relevant order is changed.

Finally, let us note that the finite-temperature approach assumes implicitly a contract of the system with thermal reservoir, i.e., with thermal, Markovian noise. Thus, the behavior observed is just the example of the classical scaling recovery for sufficiently large temperature studied in detail recently for a more general case of an arbitrary Markovian noise [22].

VII. COLD-ATOM IMPLEMENTATION

In this section, we discuss the possible implementation of the ferromagnetic Heisenberg Hamiltonian Eq. (21). We consider the system of ultracold bosons trapped in the quasi-1D optical lattice subject to a periodic driving with frequency fulfilling the resonance condition [94–97]

$$\mathcal{N}\omega = (E_p - E_s) + \mathfrak{d}, \tag{30}$$

where $\mathfrak{d}$ is a small detuning from the transition between levels (bands) with energies E_p and E_s. The dynamics of the system is captured within the two-band Bose–Hubbard model,

$$\hat{H}_0 = -\sum_{\langle i,j\rangle}(J_s \hat{s}_i^\dagger \hat{s}_j + J_p \hat{p}_i^\dagger \hat{p}_j) + \sum_i (E_s \hat{n}_i^s + E_p \hat{n}_i^p) + \hat{H}_{\rm int},$$

where J_s and J_p are tunnelings in s and p bands, respectively, and the on-site repulsive interactions are accounted for by

$$\hat{H}_{\rm int} = \sum_i \left[\frac{U_{ss}}{2}\hat{n}_i^s(\hat{n}_i^s - 1) + \frac{U_{pp}}{2}\hat{n}_i^p(\hat{n}_i^p - 1) + \frac{U_{sp}}{2}\hat{n}_i^s\hat{n}_i^p\right]. \tag{31}$$

The horizontal lattice shaking modifies the Hamiltonian by the term

$$\hat{H}_{\rm hor}(t) = \cos(\omega t) K \sum_i i(\hat{n}_i^s + \hat{n}_i^p) + J\cos(\omega t)\sum_{\langle i,j\rangle}\hat{p}_i^\dagger \hat{s}_j + W\cos(\omega t)\sum_i \hat{p}_i^\dagger \hat{s}_i + \text{H.c.}, \tag{32}$$

where the constants K, J, W depend on the amplitude of the periodic driving. The modulation of the intensity of the laser field forming the optical lattice causes the on-site energies to oscillate with amplitudes Δ_s and Δ_p at frequency ω_v.

$$\hat{H}_{\rm ver}(t) = \cos(\omega_v t)\sum_i (\Delta_s \hat{n}_i^s + \Delta_p \hat{n}_i^p). \tag{33}$$

We shall assume $\omega_v = \omega$ in the following for simplicity. The long-time dynamics of the system $H_0 + H_{\rm hor}(t) + H_{\rm ver}(t)$ with $\mathcal{N} = 3$ is described by the effective time-averaged Hamiltonian:

$$\hat{H}_{\rm eff} = \sum_i [J_{sp}^+(\hat{p}_i^\dagger \hat{s}_{i+1} + \hat{p}_i \hat{s}_{i+1}^\dagger) + J_{sp}^-(\hat{p}_{i+1}^\dagger \hat{s}_i + \hat{p}_{i+1}\hat{s}_i^\dagger)] + \sum_{\langle i,j\rangle}(J_s^{\rm ren}\hat{s}_i^\dagger \hat{s}_j + J_p^{\rm ren}\hat{p}_i^\dagger \hat{p}_j) + W_{sp}\sum_i(\hat{p}_i^\dagger \hat{s}_i + \hat{p}_i \hat{s}_i^\dagger) + \hat{H}_{\rm int}. \tag{34}$$

The intraband tunneling amplitudes are effectively $J_{s,p}^{\rm ren} = \mathcal{J}_0(K/\omega)J_{s,p}$, where $\mathcal{J}_0(x)$ is a zero-order Bessel function [82,87,97]. Similarly, the shaking-induced interband tunnelings are renormalized by factors dependent on higher-order Bessel functions yielding $J_{sp}^{\pm}$ and W_{sp} [98]. Finally, the energies of the s and p states differ only by the detuning $\mathfrak{d}$. It is now assumed that $K/\omega = x_0 + \epsilon$ (with $|\epsilon| \ll x_0$), where x_0 is the first zero of $\mathcal{J}_0$, so that the hopping within the s and p bands is strongly suppressed.

We are interested in the physics of excitations close to the ground state of Eq. (34) with the unit filling in the strongly interacting regime. The Hamiltonian $\hat{H}_{\rm eff}$, within the second order of perturbation calculus, becomes $\hat{H} = -\hat{P}_g \hat{H}_{\rm eff}(\hat{P}_e \hat{H}_{\rm eff}\hat{P}_e - E)^{-1}\hat{H}_{\rm eff}\hat{P}_g$, where $\hat{P}_g$ projects on the subspace of singly occupied states and $\hat{P}_e = 1 - \hat{P}_g$. The condition $\hat{n}_i^s + \hat{n}_i^p = 1$, which holds in the low-energy subspace, enables one to define a spin-1/2 degree of freedom at each lattice site leading to Hamiltonian Eq. (21) with $\lambda \propto W_{sp} \propto [(\Delta_p - \Delta_s)/\omega]^2$ and parameter J_z depending on the values of ϵ and $\mathfrak{d}$. Then the spin system in Eq. (21) effectively describes the excitations in the Mott space of the both laterally and vertically shaken optical lattice.

VIII. CONCLUSIONS

Let us summarize our findings. We discuss two approaches to quantum estimation of a parameter, approaches that give seemingly different predictions. This difference becomes apparent close to the critical phase transition points. In the first approach, referred to as a rotation scenario, the system is compared with its copy rotated by the parameter-dependent dynamics. The ultimate limit in this case is known as the Heisenberg limit. The second approach relies on the overlap of ground states of the system at slightly different values of the parameter. Here one may often arrive at an apparent super-Heisenberg scaling close to criticality.

The main result of our work is to provide a unified picture that links these two approaches. The necessary ingredient is an observation that the physical comparison of ground states at different parameter values can be operationally realized in an adiabatic evolution only. Under this assumption we provide an argument that both approaches yield essentially the same scaling, consistent with the Heisenberg limit when this time factor is taken into account. In effect, we obtain a straightforward generalization of the argument of Refs. [11–15], valid for time-independent systems, to an adiabatic evolution.

Importantly, our finding should hold for a broad class of a quantum many-body systems (in one or more spacial dimensions), with a particular focus on the second-order quantum critical points. As a by-product we identify the optimal observable that reveals the optimal scaling in the adiabatic limit—it is identified as a part of the Hamiltonian coupled to the parameter [i.e., H_1 in Eq. (10)].

The general result has been confirmed in a detailed study of the ferromagnetic Heisenberg Hamiltonian. On one side it forms a "minimal" Hamiltonian that reveals an apparent super-Heisenberg scaling with global magnetization as the optimal observable. We show that this "super-Heisenberg" behavior is quite robust with respect to detuning from the critical point as well as temperature. Yet, as verified in our numerical study, the time needed for measurement of the overlap (i.e., performing the necessary time evolution) leads to the recovery of the Heisenberg scaling in total agreement with the rotation scenario.

The standard metrological approach claims that the scaling may grow with the range of the interaction involving the unknown parameter [10]; i.e., super-Heisenberg behavior is in general possible if we replace the one-body operators in Eq. (10) by multiple many-body terms. However, that may reduce the possible gap in the system and therefore affect the time needed to physically realize the ground states the fidelity of which is supposed to be measured. The viewpoint developed here is that any super-Heisenberg claim must be accompanied by a careful analysis not only of system size scaling but also the time needed to prepare a given measurement.

Specifically, cold atomic systems offer direct measurements of the fidelity susceptibility without necessity of the unitary rotation by means of the Bragg spectroscopy. That may allow one to break the "unitary rotation paradigm," although careful analysis of a specific experiment is needed before giving the definite answer. In particular, high-frequency resolution in Bragg spectroscopy and the importance of low frequencies for fidelity susceptibility necessitates a sufficiently long time of measurement. The discussion of that point is beyond the scope of the present paper. Similar remarks may be addressed to "swap measurement" (see the Appendix, where this idea is developed) that also does not involve "unitary rotation." So, while we have not provided all the answers, leaving some place for future investigations, we believe that we are able to at least understand the apparent discrepancy between the unitary rotation approach and fidelity susceptibility behavior at criticality.

ACKNOWLEDGMENTS

We are grateful to Bogdan Damski and Jacek Dziarmaga for numerous discussions and hints. P. S. and J. Z. acknowledge support by PL-Grid Infrastructure and EU H2020-FETPROACT-2014 Project QUIC, while P. H. acknowledges the support of the ERC AdG QOLAPS project. This research has been supported by National Science Centre (Poland) under Projects No. 2011/01/B/ST2/05459 (P. H.), No. 2015/19/B/ST2/01028 (P. S.), No. 2016/21/B/ST2/01086 (J. Z.), and No. 2013/09/B/ST3/00239 (M. M. R.).

APPENDIX: UNIVERSAL QUADRATIC ESTIMATOR FOR PURE STATES

Consider an arbitrary Hamiltonian $\hat{H}(\lambda)$ and suppose that we have significant reasons to believe that λ is critical, but for technical reasons it is difficult to prove it. In particular, there is no linear estimator known—like the two observables discussed in the main text—that could provide an accuracy close to the limit of Fisher information scaling. The question is whether there is any way to design an experiment that would allow one to circumvent the above difficulty. To answer this affirmatively, we shall provide a simple estimator, quadratic in terms of the interaction involved, which, however, remains relatively simple and, at least in principle, can be detected with the present state-of-the-art technology of optical lattices.

Let us assume that apart from $|\Psi(\lambda+\delta_\lambda)\rangle$, experimentalist can also prepare the state at the critical point $|\Psi(\lambda)\rangle$. Now, it is known that $\mathcal{F}^2$—the square of fidelity in Eq. (9) between the two above states—can be detected using the so-called universal quantum estimator [99,100], which is measurable involving at most quadratic interaction among elementary qubits corresponding to the series of independent Hong-Ou-Mandel-type measurements [101]. The main idea behind it is to measure the quantity $\mathrm{Tr}(\hat{\rho}\,\hat{\sigma})$, which is the mean value of the *swap* observable (defined below) jointly measured on the product state $\hat{\rho}\otimes\hat{\sigma}$. The first experiment of this type was performed a relatively long time ago on two copies of the same state of the polarization-entangled photon pairs, which aimed at estimation of Rényi-2 entropy to show that violation of a suitable inequality can serve as an entanglement detector [102].

Consider the swap operator $\hat{S}$, which by definition acts as $\hat{S}|i\rangle|j\rangle = |j\rangle|i\rangle$ on $\mathcal{H}\otimes\mathcal{H}$. Alternatively, it can be represented as

$$\hat{S} = \hat{\mathbb{1}}_{\mathcal{H}}\otimes\hat{\mathbb{1}}_{\mathcal{H}} - 2\hat{P}^{\mathrm{asym}}{}_{\mathcal{H}\otimes\mathcal{H}}, \tag{A1}$$

where $\hat{P}^{\mathrm{asym}}$ is the projector on the antisymmetric subspace of $\mathcal{H} \otimes \mathcal{H}$. Then the obvious observable which measures $\mathcal{F}^2$ is

$$\hat{A}_{\mathrm{swap}} = \hat{S}^{\otimes N} = \hat{\mathbb{1}}_{\mathcal{H}^{\otimes N}} \otimes \hat{\mathbb{1}}_{\mathcal{H}^{\otimes N}} - 2\hat{P}^{\mathrm{asym}}_{\mathcal{H}^{\otimes N} \otimes \mathcal{H}^{\otimes N}} \tag{A2}$$

acting on the "quadratic" state $|\Phi\rangle = |\Psi(\lambda)\rangle \otimes |\Psi(\lambda + \delta_\lambda)\rangle$ composed of $2N$ elementary subsystems, where each $\hat{S}$ acts on one element of, respectively, first and second pure states. The above measurement corresponds to coupling each elementary subsystem of the first chain of N spins with the corresponding subsystem of the second chain and performing the measurement by projecting it on the antisymmetric subspace and then multiplying the results. This gives the overall results of $+1$ (-1) when the number of successive projections is even (odd).

Now it is an elementary exercise to see that in this case the error propagation formula of Eq. (3) takes the form

$$\Delta_{\delta_\lambda}(\hat{A}_{\mathrm{swap}}, \lambda) = \frac{1}{\sqrt{2\chi_F(\lambda)}} = \sqrt{\frac{2}{G(\lambda)}}, \tag{A3}$$

where we employ Eq. (8) and $\hat{A}^2_{\mathrm{swap}} = \hat{\mathbb{1}}$. The error propagation formula in Eq. (A3) is then only by a factor of 2 worse than the best possible linear estimator. Therefore, we get a quadratic estimator that reproduces —up to the constant factor—the scaling in N of the best possible linear one. Note that applying the above procedure to the original unitary perturbation scheme (like in, e.g., Refs. [9,27,43]) cannot surpass the Heisenberg limit, since the whole scheme may be simulated as a measurement of some new observable on the $|\Psi(\lambda)\rangle$ alone, which is known to obey the limit as long as the part of the Hamiltonian with unknown parameter λ is fully local; see Refs. [13,14,16].

Now the question is, can we employ the above approach for the case of bosonic lattices considered in Sec. VII? Fortunately, the answer is, at least in principle, affirmative. Indeed, very recently it has been shown how to directly perform the measurement of the swap observable on the bosonic lattices [103–106] where the authors designed the beam splitter type of interaction as a tunneling coupling between two optical lattices, followed by the measurement of the parity of the on-site occupation numbers. This guarantees that the observable in Eq. (A2), which is crucial for the experimental application of the formula Eq. (A3), can be directly measured on the optical system with an effective spin Hamiltonian having the critical parameter introduced by lattice shaking.

[1] C. M. Caves, *Quantum-Mechanical Noise in an Interferometer*, Phys. Rev. D **23**, 1693 (1981).

[2] D. J. Wineland, J. J. Bollinger, W. M. Itano, F. L. Moore, and D. J. Heinzen, *Spin Squeezing and Reduced Quantum Noise in Spectroscopy*, Phys. Rev. A **46**, R6797 (1992).

[3] S. L. Braunstein and C. M. Caves, *Statistical Distance and the Geometry of Quantum States*, Phys. Rev. Lett. **72**, 3439 (1994).

[4] V. Giovannetti, S. Lloyd, and L. Maccone, *Quantum-Enhanced Measurements: Beating the Standard Quantum Limit*, Science **306**, 1330 (2004).

[5] A. Uhlmann, *The "Transition Probability" in the State Space of a *-Algebra*, Rep. Math. Phys. **9**, 273 (1976).

[6] M. M. Taddei, B. M. Escher, L. Davidovich, and R. L. de Matos Filho, *Quantum Speed Limit for Physical Processes*, Phys. Rev. Lett. **110**, 050402 (2013).

[7] V. Giovannetti, S. Lloyd, and L. Maccone, *Advances in Quantum Metrology*, Nat. Photonics **5**, 222 (2011).

[8] G. Tóth and I. Apellaniz, *Quantum Metrology from a Quantum Information Science Perspective*, J. Phys. A **47**, 424006 (2014).

[9] R. Demkowicz-Dobrzanski, M. Jarzyna, and J. Kolodynski, *Quantum Limits in Optical Interferometry*, Prog. Opt. **60**, 345 (2015).

[10] S. M. Roy and S. L. Braunstein, *Exponentially Enhanced Quantum Metrology*, Phys. Rev. Lett. **100**, 220501 (2008).

[11] S. Boixo, S. T. Flammia, C. M. Caves, and J. M. Geremia, *Generalized Limits for Single-Parameter Quantum Estimation*, Phys. Rev. Lett. **98**, 090401 (2007).

[12] V. Giovannetti, S. Lloyd, and L. Maccone, *Quantum Metrology*, Phys. Rev. Lett. **96**, 010401 (2006).

[13] A. De Pasquale, D. Rossini, P. Facchi, and V. Giovannetti, *Quantum Parameter Estimation Affected by Unitary Disturbance*, Phys. Rev. A **88**, 052117 (2013).

[14] M. Skotiniotis, P. Sekatski, and W. Dür, *Quantum Metrology for the Ising Hamiltonian with Transverse Magnetic Field*, New J. Phys. **17**, 073032 (2015).

[15] S. Pang and T. A. Brun, *Quantum Metrology for a General Hamiltonian Parameter*, Phys. Rev. A **90**, 022117 (2014).

[16] J. M. E. Fraisse and D. Braun, *Hamiltonian Extensions in Quantum Metrology*, Quantum Meas. Quantum Metrol. **4**, 8 (2017).

[17] R. Demkowicz-Dobrzanski, J. Kołodyński, and M. Guta, *The Elusive Heisenberg Limit in Quantum Enhanced Metrology*, Nat. Commun. **3**, 1063 (2012).

[18] S. Alipour, M. Mehboudi, and A. T. Rezakhani, *Quantum Metrology in Open Systems: Dissipative Cramér-Rao Bound*, Phys. Rev. Lett. **112**, 120405 (2014).

[19] S. Alipour and A. T. Rezakhani, *Extended Convexity of Quantum Fisher Information in Quantum Metrology*, Phys. Rev. A **91**, 042104 (2015).

[20] A. Chenu, M. Beau, J. Cao, and A. del Campo, *Quantum Simulation of Generic Many-Body Open System Dynamics Using Classical Noise*, Phys. Rev. Lett. **118**, 140403 (2017).

[21] M. Beau and A. del Campo, *Nonlinear Quantum Metrology of Many-Body Open Systems*, Phys. Rev. Lett. **119**, 010403 (2017).

[22] R. Demkowicz-Dobrzański, J. Czajkowski, and P. Sekatski, *Adaptive Quantum Metrology under General Markovian Noise*, Phys. Rev. X **7**, 041009 (2017).

[23] P. Hyllus, W. Laskowski, R. Krischek, C. Schwemmer, W. Wieczorek, H. Weinfurter, L. Pezzé, and A. Smerzi, *Fisher Information and Multiparticle Entanglement*, Phys. Rev. A **85**, 022321 (2012).

[24] G. Tóth, *Multipartite Entanglement and High-Precision Metrology*, Phys. Rev. A **85**, 022322 (2012).

[25] R. Augusiak, J. Kołodyński, A. Streltsov, M. N. Bera, A. Acín, and M. Lewenstein, *Asymptotic Role of Entanglement in Quantum Metrology*, Phys. Rev. A **94**, 012339 (2016).

[26] Ł. Czekaj, A. Przysiężna, M. Horodecki, and P. Horodecki, *Quantum Metrology: Heisenberg Limit with Bound Entanglement*, Phys. Rev. A **92**, 062303 (2015).

[27] P. Hauke, M. Heyl, L. Tagliacozzo, and P. Zoller, *Measuring Multipartite Entanglement through Dynamic Susceptibilities*, Nat. Phys. **12**, 778 (2016).

[28] I. Apellaniz, M. Kleinmann, O. Gühne, and G. Tóth, *Optimal Witnessing of the Quantum Fisher Information with Few Measurements*, Phys. Rev. A **95**, 032330 (2017).

[29] P. T. Ernst, S. Gotze, J. S. Krauser, K. Pyka, D.-S. Luhmann, D. Pfannkuche, and K. Sengstock, *Probing Superfluids in Optical Lattices by Momentum-Resolved Bragg Spectroscopy*, Nat. Phys. **6**, 56 (2010).

[30] D. Clément, N. Fabbri, L. Fallani, C. Fort, and M. Inguscio, J. Low Temp. Phys. **158**, 5 (2010).

[31] M. Tsang, *Quantum Transition-Edge Detectors*, Phys. Rev. A **88**, 021801 (2013).

[32] T. Macrì, A. Smerzi, and L. Pezzè, *Loschmidt Echo for Quantum Metrology*, Phys. Rev. A **94**, 010102 (2016).

[33] U. Marzolino and T. Prosen, *Quantum Metrology with Nonequilibrium Steady States of Quantum Spin Chains*, Phys. Rev. A **90**, 062130 (2014).

[34] U. Marzolino and T. Prosen, *Computational Complexity of Nonequilibrium Steady States of Quantum Spin Chains*, Phys. Rev. A **93**, 032306 (2016).

[35] M. A. Rajabpour, *Multipartite Entanglement and Quantum Fisher Information in Conformal Field Theories*, Phys. Rev. D **96**, 126007 (2017).

[36] D. Braun, G. Adesso, F. Benatti, R. Floreanini, U. Marzolino, M. W. Mitchell, and S. Pirandola, *Quantum Enhanced Measurements without Entanglement*, arXiv:1701.05152 [Rev. Mod. Phys. (to be published)].

[37] P. Zanardi and N. Paunković, *Ground State Overlap and Quantum Phase Transitions*, Phys. Rev. E **74**, 031123 (2006).

[38] W.-L. You, Y.-W. Li, and S.-J. Gu, *Fidelity, Dynamic Structure Factor, and Susceptibility in Critical Phenomena*, Phys. Rev. E **76**, 022101 (2007).

[39] P. Zanardi, M. G. A. Paris, and L. Campos Venuti, *Quantum Criticality as a Resource for Quantum Estimation*, Phys. Rev. A **78**, 042105 (2008).

[40] C. Invernizzi, M. Korbman, L. Campos Venuti, and M. G. A. Paris, *Optimal Quantum Estimation in Spin Systems at Criticality*, Phys. Rev. A **78**, 042106 (2008).

[41] G. Salvatori, A. Mandarino, and M. G. A. Paris, *Quantum Metrology in Lipkin-Meshkov-Glick Critical Systems*, Phys. Rev. A **90**, 022111 (2014).

[42] M. Bina, I. Amelio, and M. G. A. Paris, *Dicke Coupling by Feasible Local Measurements at the Superradiant Quantum Phase Transition*, Phys. Rev. E **93**, 052118 (2016).

[43] W. L. Boyajian, M. Skotiniotis, W. Dür, and B. Kraus, *Compressed Quantum Metrology for the Ising Hamiltonian*, Phys. Rev. A **94**, 062326 (2016).

[44] M. Mehboudi, L. A. Correa, and A. Sanpera, *Achieving Sub-Shot-Noise Sensing at Finite Temperatures*, Phys. Rev. A **94**, 042121 (2016).

[45] I. Frérot and T. Roscilde, *Quantum Critical Metrology*, arXiv:1707.08804.

[46] M. Hübner, *Computation of Uhlmann's Parallel Transport for Density Matrices and the Bures Metric on Three-Dimensional Hilbert Space*, Phys. Lett. A **179**, 226 (1993).

[47] L. Gong and P. Tong, *Fidelity, Fidelity Susceptibility, and von Neumann Entropy to Characterize the Phase Diagram of an Extended Harper Model*, Phys. Rev. B **78**, 115114 (2008).

[48] S.-J. Gu, H.-M. Kwok, W.-Q. Ning, and H.-Q. Lin, *Fidelity Susceptibility, Scaling, and Universality in Quantum Critical Phenomena*, Phys. Rev. B **77**, 245109 (2008).

[49] S. Greschner, A. K. Kolezhuk, and T. Vekua, *Fidelity Susceptibility and Conductivity of the Current in One-Dimensional Lattice Models with Open or Periodic Boundary Conditions*, Phys. Rev. B **88**, 195101 (2013).

[50] H.-Q. Zhou and J. P. Barjaktarevič, *Fidelity and Quantum Phase Transitions*, J. Phys. A **41**, 412001 (2008).

[51] M. M. Rams and B. Damski, *Quantum Fidelity in the Thermodynamic Limit*, Phys. Rev. Lett. **106**, 055701 (2011); *Scaling of Ground-State Fidelity in the Thermodynamic Limit: XY Model and Beyond*, Phys. Rev. A **84**, 032324 (2011).

[52] L. Campos Venuti and P. Zanardi, *Quantum Critical Scaling of the Geometric Tensors*, Phys. Rev. Lett. **99**, 095701 (2007).

[53] D. Schwandt, F. Alet, and S. Capponi, *Quantum Monte Carlo Simulations of Fidelity at Magnetic Quantum Phase Transitions*, Phys. Rev. Lett. **103**, 170501 (2009).

[54] A. F. Albuquerque, F. Alet, C. Sire, and S. Capponi, *Quantum Critical Scaling of Fidelity Susceptibility*, Phys. Rev. B **81**, 064418 (2010).

[55] A. Polkovnikov and V. Gritsev, *Universal Dynamics Near Quantum Critical Points, Understanding Quantum Phase Transitions*, arXiv:0910.3692.

[56] S Sachdev, *Quantum Phase Transitions* (Cambridge University Press, Cambridge, England, 1999).

[57] S. L. Sondhi, S. M. Girvin, J. P. Carini, and D. Shahar, *Continuous Quantum Phase Transitions*, Rev. Mod. Phys. **69**, 315 (1997).

[58] M. A. Continentino, *Quantum Scaling in Many-Body Systems* (World Scientific Publishing, Singapore, 2001).

[59] C. De Grandi, V. Gritsev, and A. Polkovnikov, *Quench Dynamics Near a Quantum Critical Point*, Phys. Rev. B **81**, 012303 (2010); *Quench Dynamics Near a Quantum Critical Point: Application to the Sine-Gordon Model*, Phys. Rev. B **81**, 224301 (2010).

[60] Y. Chen, Z. D. Wang, Y. Q. Li, and F. C. Zhang, *Spin-Orbital Entanglement and Quantum Phase Transitions in a Spin-Orbital Chain with* $\mathrm{SU}(2) \times \mathrm{SU}(2)$ *Symmetry*, Phys. Rev. B **75**, 195113 (2007).

[61] B. Damski, *Fidelity Susceptibility of the Quantum Ising Model in a Transverse Field: The Exact Solution*, Phys. Rev. E **87**, 052131 (2013); B. Damski and M. M. Rams, *Exact Results for Fidelity Susceptibility of the Quantum Ising Model: The Interplay between Parity, System Size, and Magnetic Field*, J. Phys. A **47**, 025303 (2014).

[62] S. Knysh, *Zero-Temperature Quantum Annealing Bottlenecks in the Spin-Glass Phase*, Nat. Commun. **7**, 12370 (2016).

[63] W. H. Zurek, U. Dorner, and P. Zoller, *Dynamics of a Quantum Phase Transition*, Phys. Rev. Lett. **95**, 105701 (2005).

[64] J. Dziarmaga, *Dynamics of a Quantum Phase Transition and Relaxation to a Steady State*, Adv. Phys. **59**, 1063 (2010).

[65] A. Polkovnikov, K. Sengupta, A. Silva, and M. Vengalattore, *Colloquium: Nonequilibrium Dynamics of Closed Interacting Quantum Systems*, Rev. Mod. Phys. **83**, 863 (2011).

[66] J. Cardy, *Scaling and Renormalization in Statistical Physics* (Cambridge University Press, Cambridge, England, 1996), Vol. 5.

[67] W.-L. You, Y.-W. Li, and S.-J. Gu, *Fidelity, Dynamic Structure Factor, and Susceptibility in Critical Phenomena*, Phys. Rev. E **76**, 022101 (2007).

[68] S. Deffner and S. Campbell, *Quantum Speed Limits: From Heisenberg's Uncertainty Principle to Optimal Quantum Control*, J. Phys. A **50**, 453001 (2017).

[69] Following Ref. [70] consider the cluster-Ising spin chain $H_0 = -\sum_n (2\sigma_n^z\sigma_{n+1}^z + \sigma_n^x - \sigma_n^z\sigma_{n+1}^x\sigma_{n+2}^z)$ which is critical and has the GHZ state as the ground state. Now, the relevant perturbation aligned with this state is $H_1 = -\sum_n h_n = -\sum_n \sigma_n^z$. In such a system $z = 2$ and $[h] = 0$.

[70] M. M. Wolf, G. Ortiz, F. Verstraete, and J. I. Cirac, *Quantum Phase Transitions in Matrix Product Systems*, Phys. Rev. Lett. **97**, 110403 (2006).

[71] See for instance Eqs. (7)–(9) in Ref. [14]. In Eq. (8) we allow a small change of, say, λ_1 to depend on time.

[72] I. Affleck and M. Oshikawa, *Field-Induced Gap in Cu Benzoate and Other $s = \frac{1}{2}$ Antiferromagnetic Chains*, Phys. Rev. B **60**, 1038 (1999).

[73] L. Campos Venuti and P. Zanardi, *Quantum Critical Scaling of the Geometric Tensors*, Phys. Rev. Lett. **99**, 095701 (2007).

[74] J. Sirker, *Finite-Temperature Fidelity Susceptibility for One-Dimensional Quantum Systems*, Phys. Rev. Lett. **105**, 117203 (2010).

[75] G. Sun, A. K. Kolezhuk, and T. Vekua, *Fidelity at Berezinskii-Kosterlitz-Thouless Quantum Phase Transitions*, Phys. Rev. B **91**, 014418 (2015).

[76] The experienced reader may wonder that for odd N the ground state is exactly degenerate at the critical point $\lambda_c = 0$, which leads to singularity in χ_F if one uses Eq. (9) directly. For simplicity of the discussion, we use even N in the numerics.

[77] In the perturbative regime of $t \ll 1$ it is easy to see that $\Delta_{\delta_\lambda}(\hat{H}_1, \lambda_c, t) \sim t^{-2}$. Such a region is not shown in Fig. 2.

[78] F. Verstraete, V. Murg, and J. I. Cirac, *Matrix Product States, Projected Entangled Pair States, and Variational Renormalization Group Methods for Quantum Spin Systems*, Adv. Phys. **57**, 143 (2008).

[79] U. Schollwöck, *The Density-Matrix Renormalization Group in the Age of Matrix Product States*, Ann. Phys. (Amsterdam) **326**, 96 (2011).

[80] J. Haegeman, J. I. Cirac, T. J. Osborne, I. Pižorn, H. Verschelde, and F. Verstraete, *Time-Dependent Variational Principle for Quantum Lattices*, Phys. Rev. Lett. **107**, 070601 (2011); J. Haegeman, C. Lubich, I. Oseledets, B. Vandereycken, and F. Verstraete, *Unifying Time Evolution and Optimization with Matrix Product States*, Phys. Rev. B **94**, 165116 (2016).

[81] M. Suzuki, *General Decomposition Theory of Ordered Exponentials*, Proc. Jpn. Acad. Ser. B **69**, 161 (1993); N. Hatano and M. Suzuki, *Quantum Annealing and Other Optimization Methods* (Springer, New York, 2005), pp. 37–68.

[82] A. Eckardt, C. Weiss, and M. Holthaus, *Superfluid-Insulator Transition in a Periodically Driven Optical Lattice*, Phys. Rev. Lett. **95**, 260404 (2005).

[83] A. Eckardt, P. Hauke, P. Soltan-Panahi, C. Becker, K. Sengstock, and M. Lewenstein, *Frustrated Quantum Antiferromagnetism with Ultracold Bosons in a Triangular Lattice*, Europhys. Lett. **89**, 10010 (2010).

[84] M. Łącki and J. Zakrzewski, *Fast Dynamics for Atoms in Optical Lattices*, Phys. Rev. Lett. **110**, 065301 (2013).

[85] N. Goldman and J. Dalibard, *Periodically Driven Quantum Systems: Effective Hamiltonians and Engineered Gauge Fields*, Phys. Rev. X **4**, 031027 (2014).

[86] M. Bukov, L. D'Alessio, and A. Polkovnikov, *Universal High-Frequency Behavior of Periodically Driven Systems: From Dynamical Stabilization to Floquet Engineering*, Adv. Phys. **64**, 139 (2015).

[87] A. Eckardt and E. Anisimovas, *High-Frequency Approximation for Periodically Driven Quantum Systems from a Floquet-Space Perspective*, New J. Phys. **17**, 093039 (2015).

[88] A. Dutta, G. Aeppli, B. K. Chakrabarti, U. Divakaran, T. F. Rosenbaum, and D. Sen, *Quantum Phase Transitions in Transverse Field Spin Models: From Statistical Physics to Quantum Information* (Cambridge University Press, Cambridge, England, 2015).

[89] H. T. Quan, Z. Song, X. F. Liu, P. Zanardi, and C. P. Sun, *Decay of Loschmidt Echo Enhanced by Quantum Criticality*, Phys. Rev. Lett. **96**, 140604 (2006).

[90] A. Peres, *Stability of Quantum Motion in Chaotic and Regular Systems*, Phys. Rev. A **30**, 1610 (1984).

[91] Note that here the scaling remains tight also beyond the perturbative regime of very short times.

[92] L. Campos Venuti and P. Zanardi, *Unitary Equilibrations: Probability Distribution of the Loschmidt Echo*, Phys. Rev. A **81**, 022113 (2010).

[93] V. Mukherjee, S. Sharma, and A. Dutta, *Loschmidt Echo with a Nonequilibrium Initial State: Early-Time Scaling and Enhanced Decoherence*, Phys. Rev. B **86**, 020301 (2012).

[94] C. Sträter and A. Eckardt, *Orbital-Driven Melting of a Bosonic Mott Insulator in a Shaken Optical Lattice*, Phys. Rev. A **91**, 053602 (2015).

[95] A. Przysiężna, O. Dutta, and J. Zakrzewski, *Rice-Mele Model with Topological Solitons in an Optical Lattice*, New J. Phys. **17**, 013018 (2015).

[96] O. Dutta, A. Przysiężna, and J. Zakrzewski, *Spontaneous Magnetization and Anomalous Hall Effect in an Emergent Dice Lattice*, Sci. Rep. **5**, 11060 (2015).

[97] A. Eckardt, *Colloquium: Atomic Quantum Gases in Periodically Driven Optical Lattices*, Rev. Mod. Phys. **89**, 011004 (2017).

[98] P. Sierant, O. Dutta, and J. Zakrzewski, *Effective Spin Models from Cold Bosons in Optical Shaken Potentials* (to be published).

[99] A. K. Ekert, C. M. Alves, D. K. L. Oi, M. Horodecki, P. Horodecki, and L. C. Kwek, *Direct Estimations of Linear and Nonlinear Functionals of a Quantum State*, Phys. Rev. Lett. **88**, 217901 (2002).

[100] P. Horodecki and A. Ekert, *Method for Direct Detection of Quantum Entanglement*, Phys. Rev. Lett. **89**, 127902 (2002).

[101] J. A. Miszczak, Z. Puchała, P. Horodecki, A. Uhlmann, and K. Życzkowski, *Sub- and Super–Fidelity as Bounds for Quantum Fidelity*, Quantum Inf. Comput. **9**, 0103 (2009).

[102] F. A. Bovino, G. Castagnoli, A. Ekert, P. Horodecki, C. M. Alves, and A. V. Sergienko, *Direct Measurement of Nonlinear Properties of Bipartite Quantum States*, Phys. Rev. Lett. **95**, 240407 (2005).

[103] A. J. Daley, H. Pichler, J. Schachenmayer, and P. Zoller, *Measuring Entanglement Growth in Quench Dynamics of Bosons in an Optical Lattice*, Phys. Rev. Lett. **109**, 020505 (2012).

[104] H. Pichler, L. Bonnes, A. J. Daley, A. M. Läuchli, and P. Zoller, *Thermal versus Entanglement Entropy: A Measurement Protocol for Fermionic Atoms with a Quantum Gas Microscope*, New J. Phys. **15**, 063003 (2013).

[105] A. Elben, B. Vermersch, M. Dalmonte, J. I. Cirac, and P. Zoller, *Rényi Entropies from Random Quenches in Atomic Hubbard and Spin Models*, Phys. Rev. Lett. **120**, 050406 (2018).

[106] B. Vermersch, A. Elben, M. Dalmonte, J. I. Cirac, and P. Zoller, *Unitary n-Designs via Random Quenches in Atomic Hubbard and Spin Models: Application to the Measurement of Rényi Entropies*, Phys. Rev. A **97**, 023604 (2018).